AIMS Mathematics

https://www.aimspress.com/journal/Math

AIMS Mathematics, 11(9): 28991–29021.
DOI:10.3934/math.20261153
Received: 13 May 2026
Revised: 10 August 2026
Accepted: 19 August 2026
Published: 09 September 2026

*Research article*

# Mean-square exponential synchronization of coupled neural networks with non-Markovian noise via adaptive control

**Zixin Zhu**[1], **Weihua Wan**[2], **Yuming Feng**[3,*] **and Xiangguang Dai**[3]

[1] School of Mathematics and Statistics, Chongqing Sanxia University of Science and Technology, Wanzhou, Chongqing 404100, China

[2] School of Intelligent Technology, Chongqing Preschool Education College, Wanzhou, Chongqing 404047, China

[3] School of Computer Science and Engineering of Science and Engineering, Chongqing Sanxia University of Science and Technology, Wanzhou, Chongqing 404100, China

* **Correspondence:** Email: yumingfeng25928@163.com.

**Abstract:** In this paper, we investigated the synchronization problem of neural networks under non-Markovian disturbances. By incorporating fractional Brownian motion (fBm) and Markovian switching, the proposed model could characterize long-memory effects in stochastic systems. A hybrid adaptive control strategy, including gain adjustment, memory-kernel feedback, and distributed compensation, was developed to achieve synchronization. Sufficient conditions for mean-square exponential stability were derived using a Lyapunov functional approach. Numerical results showed that the proposed controller achieved a settling time of $0.91s$, compared with $3.75s$, $4.55s$, and $7.99s$ for the the Linear Feedback Controller (LFC), Proportional-Derivative (PD), and Proportional-Integral-Derivative (PID) controllers, respectively, while achieving smaller Integral Square Error (ISE), Integral Absolute Error (IAE), and Integral Time Absolute Error (ITAE) values.

**Keywords:** non-Markovian dynamics; dynamic adaptation; mean square exponential stability; fractional Brownian motion
**Mathematics Subject Classification:** 60H10, 93C10, 93D20

## 1. Introduction

With the development of artificial intelligence, neuroscience, and network control, synchronization has become a fundamental research topic in complex dynamical networks and has attracted considerable attention [1–3]. Synchronization of neural networks is particularly important in information processing, secure communication, and complex network systems. Traditional neural network models are mainly based on deterministic systems or Markovian stochastic perturbations [4,5]. Nevertheless, disturbances in many practical systems may exhibit long-memory, state-dependent, and non-Markovian characteristics. Such phenomena can be found in biological neural networks, financial systems [6, 7], and intelligent transportation systems [8, 9]. These complex disturbance characteristics create new difficulties for system modeling, stability analysis, and controller design.

Recent studies have used graph-based and spatio-temporal learning methods to capture complex spatial and temporal patterns in dynamic networked systems [10, 11]. Other recent works have extended these models by considering more advanced computational frameworks and multimodal information [12, 13]. Although these approaches are effective for data-driven prediction, they mainly address forecasting tasks rather than the stability and synchronization of stochastic dynamical systems.

Synchronization and stability of Markovian jumping systems have been extensively studied in recent years [14–16]. Wang et al. [17] investigated synchronization criteria for delayed inertial neural networks with generally Markovian jumping. Sampled-data synchronization of Markov jump delayed neural networks was also studied in [18]. The memoryless nature of Markovian processes limits their ability to describe disturbances with long-range dependence. Time-varying delays have therefore been considered in neural network models to describe delayed interactions [19–21]. Some related works have also investigated relaxed Lyapunov functionals and sampled-data schemes [22, 23], as well as feedback and adaptive control methods for synchronization and robustness [24, 25]. However, these results are mainly concerned with deterministic disturbances, white noise, or standard Brownian motion. The synchronization problem under stochastic disturbances with long-range memory and non-Markovian characteristics has received comparatively less attention.

Some researchers have extended stochastic system analysis to more complex disturbances. Wu et al. [26] investigated time-varying delayed stochastic differential systems with non-Markovian switching parameters. Tiwari and Senapati [27] considered stochastic systems with memory-related effects. These researches extend the traditional Markovian framework. Despite this, fractional Brownian motion (fBm) and intermittent disturbances are not simultaneously considered in these frameworks.

The fBm provides an effective way to describe long-memory stochastic behavior. Unlike standard Brownian motion, fBm has long-range dependence and self-similarity. It has therefore been used to model complex stochastic dynamics [28, 29]. Fractional-order models have also shown good ability to describe memory and hereditary properties [30, 31]. In particular, Liaqat et al. [32] studied fractional stochastic systems driven by fBm with a general memory kernel. Even so, state-dependent disturbance intensity and intermittent disturbance activation were not simultaneously considered.

Intermittent disturbances are another important factor in stochastic network systems. Such disturbances are activated only during certain time intervals or events. Existing studies have considered impulsive [33, 34] and event-driven mechanisms [35–37]. Intermittent control has also been applied to the synchronization of fractional-order chaotic neural networks [38]. Zhou et al. [39] investigated the synchronization of coupled neural networks with intermittent random disturbances. Intermittent control has also been used to reduce control energy [40] and to describe pulse-driven control processes [41]. Yet long-memory stochastic effects generated by fBm were not considered in that model.

Advanced control strategies have also been developed for nonlinear networked systems. For example, fuzzy-based $H_\infty$ consensus control under sampled-data mechanisms has been investigated to improve robustness against uncertainties and communication constraints [42]. Adaptive control provides another useful approach to neural network synchronization. Adaptive neural network controllers and event-triggered control strategies for networked systems have been developed in [43–45]. Memory-based adaptive control for stochastic neural networks have been explored in [46], but non-Markovian long-memory effects, fBm, and state-dependent intermittent disturbances have not been considered simultaneously.

To further clarify the differences between our work and the representative existing studies, Table 1 compares several approaches in terms of intermittent disturbances, non-Markovian/fBm characteristics, memory effects, and adaptive control.

**Table 1.** Comparison with representative state-of-the-art studies.

| Reference | Intermittent disturbance | Non-Markovian/fBm characteristics | Memory effect | Adaptive control |
|---|---|---|---|---|
| [39] | ✓ | – | – | – |
| [26] | – | ✓ | – | – |
| [32] | – | ✓ | ✓ | – |
| **This paper** | ✓ | ✓ | ✓ | ✓ |

In this table, '✓' signifies that the respective reference takes the corresponding factor into account, and '–' indicates the absence of that factor in the reported design.

As shown in Table 1, although representative studies have addressed intermittent disturbances, non-Markovian dynamics, and memory effects from different perspectives, these mechanisms have mainly been investigated under separate frameworks. Their combined effects on the synchronization of coupled neural networks remain insufficiently explored. In particular, the simultaneous presence of long-memory, state-dependent, and intermittently activated stochastic disturbances creates additional difficulties for stability analysis and controller design.

Motivated by these limitations, an adaptive non-Markovian perturbation model for coupled neural networks is developed. An fBm is introduced to describe long-range dependence, while a memory kernel is used to characterize the influence of historical disturbance information. A state-dependent disturbance intensity is introduced to describe variations in disturbance strength. An intermittent mechanism is further incorporated to represent randomly activated disturbances. In this way, the proposed model combines these stochastic characteristics within a unified framework.

These disturbance characteristics also make conventional controller design more difficult. Fixed-gain controllers cannot adjust the control strength according to changes in synchronization errors, while memoryless controllers do not explicitly use historical information to compensate for long-memory disturbances. Therefore, an adaptive memory controller is developed. The adaptive mechanism adjusts the control gains according to the synchronization errors, while the memory term uses historical state information to compensate for long-memory perturbations. Thus, the controller design is directly motivated by the characteristics of the proposed non-Markovian disturbance model.

Based on the above motivation and research gaps, the main contributions of this paper are summarized as follows:

1) For the response system, a new class of dynamic adaptive non-Markovian disturbance model is established, and the adaptive disturbance intensity function and fBm integral are introduced to break through the short-term memory limitation of traditional Markov noise.

2) A hybrid adaptive controller is designed, which includes three collaborative mechanisms: state-sensitive gain adjustment, memory kernel integral feedback, and distributed coupling compensation.
3) By using a new Lyapunov functional in combination with fractional Malliavin calculus, mean-square stability is established of the error system.

The remainder of this paper is organized as follows. In Section 2, we introduce the necessary preliminaries. In Section 3, we present the adaptive non-Markovian perturbation model and the coupled neural network system. In Section 4, we develop the adaptive memory controller and establish the main synchronization results. In Section 5, we present numerical simulations and comparative experiments. Finally, In Section 6, we conclude the paper and discuss possible future research directions.

## 2. Preliminaries

**Notations:** We adopt the standard notation of $\mathbb{R}$ for the real numbers and $\mathbb{R}^n$ for the Euclidean $n$-space. We denote the transpose of matrix $M$ by $M^T$. Let $v = [v_1, v_2, \cdots, v_n]^T \in \mathbb{R}^n$ be an arbitrary vector, and we define its 2-norm as $\|v\|^2 = \sum_{i=1}^{n} v_i^2$. Operator $E(\cdot)$ represents the mathematical expectation. $I_m$ denotes the identity matrix of order $m$. $B^H(t) = [B_1^H(t), B_2^H(t), \cdots, B_m^H(t)]^T$ is a standard fBm and $H \in (0, 1)$, while $B^1(t) = [B_1^1(t), B_2^1(t), \cdots, B_m^1(t)]^T$ and $B^2(t) = [B_1^2(t), B_2^2(t), \cdots, B_m^2(t)]^T$ are $m$-dimensional Brownian motions.

**Assumption 1** ( [39]). *Given two distinct real numbers $\xi_1, \xi_2 \in \mathbb{R}$, the activation functions $\check{\eta}(\cdot)$ and $\check{\mu}(\cdot)$ in* (3.3) *and* (3.4) *are continuous and bounded. Specifically, for positive constants $k_1$ and $k_2$, we have the inequality*

$$0 \le \frac{\check{\eta}(\xi_1) - \check{\eta}(\xi_2)}{\xi_1 - \xi_2} \le k_1, \quad 0 \le \frac{\check{\mu}(\xi_1) - \check{\mu}(\xi_2)}{\xi_1 - \xi_2} \le k_2. \tag{2.1}$$

**Assumption 2.** *The memory kernel $K(t, s) = \dfrac{(t-s)^{\alpha-1} e^{-\lambda(t-s)}}{\Gamma(\alpha)}$ and the fractional noise correlation $\iota_H(t, s) = H(2H - 1)|t - s|^{2H-2}$ satisfy the following*

*1) $K(t, s) > 0$ for all $0 \le s < t$.*
*2) Assume we have two positive constants $\kappa_1, \kappa_2 > 0$ satisfying*

$$\int_0^t K(t, s)\, ds \le \kappa_1, \quad \int_0^t K^2(t, s)\, ds \le \kappa_2.$$

*This ensures that the kernel is non-degenerate, bounded, and integrable, which is essential for the Lyapunov integral terms to be well defined and finite.*

*3) The integral $\int_0^t K(t, s)\iota_H(t, s)\, ds$ converges, with the constraint on parameters below*

$$\alpha + 2H > 2.$$

**Remark 1.** *The condition $\alpha + 2H > 2$ guarantees the integrability of the kernel–fractional noise interaction term, ensuring that the memory-related stochastic integral remains finite in the mean-square sense.*

**Assumption 3.** *The state-related disturbance gain function $\sigma_i(t)$ and $\gamma_i(t)$ is bounded, and positive constants $\sigma_{\max} > 0$ and $\gamma_{\max} > 0$ satisfying*

$$\sigma_i(t) \leq \sigma_{\max}, \quad \gamma_i(t) \leq \gamma_{\max}, \quad \forall t \geq 0. \tag{2.2}$$

**Assumption 4.** *The internal disturbance intensity function $D_i(t)$ is bounded, and there is a $D_{max} > 0$ satisfying $D_i(t) \leq D_{\max}, \forall t \geq 0$.*

**Assumption 5.** *The Gaussian weight function $W(t,s) = \frac{e^{-\rho(t-s)}}{\sqrt{2\pi\zeta^2}} \exp\left(-\frac{(t-s)^2}{2\zeta^2}\right)$ is uniformly bounded for all $t \geq s$, i.e.,*

$$|W(t,s)| \leq \frac{1}{\sqrt{2\pi\zeta^2}} = W_{max},$$

*where $\rho > 0$ and $\zeta > 0$.*

**Remark 2.** *Assumption 1 ensures the Lipschitz continuity of the neuron activation functions, which is essential for controlling the growth of nonlinear interactions in the network. Assumption 2 guarantees that the memory kernel and fractional noise correlation are integrable, preventing the integral terms from diverging and ensuring well-posedness of the system dynamics. Assumptions 3 and 4 restrict the disturbance intensity to a bounded domain, which is necessary for the mean-square boundedness and stability analysis in the stochastic system under external uncertainties. Assumption 5 further prevents the delay-related integral term from growing unbounded and guarantees that the contribution of past states remains finite, thereby supporting the convergence of Lyapunov-based stability arguments.*

**Definition 1** ( [47]). *H represents the Hurst parameter, which is $H \in (0,1)$. The essential properties of an fBm, with H denoting the Hurst parameter, are that it is a Gaussian process and its sample paths are continuous, satisfying the equation*

$$\mathbb{E}[B^H(t)B^H(s)] = \frac{1}{2}\left(|t|^{2H} + |s|^{2H} - |t-s|^{2H}\right), \forall t, s \in \mathbb{R}.$$

*By Definition 1, the $B^H(t)$ meets the conditions below*

1) $B^H(0) = 0$ *and* $\mathbb{E}[B^H(t)] = 0$ *for* $t \geq 0$.
2) $dB^H(t) = B^H(t+dt) - B^H(t),\ dt \geq 0$.

**Remark 3.** *The behavior of the fBm is dictated by its Hurst parameter H in the following:*

1) *At $H = 0.5$, the process degenerates to standard Brownian motion, possessing uncorrelated increments.*
2) *For $H > 0.5$, this is a long-memory process whose increments display positive dependence.*
3) *For $H < 0.5$, this is an anti-persistent process, marked by negatively autocorrelated increments.*

**Definition 2** ( [48]). *Let $B^H = \{B^H(t), t \geq 0\}$ be an fBm with $H \in (\frac{1}{2}, 1)$. For a smooth cylindrical random variable*

$$F = f\left(B^H(\varphi_1), B^H(\varphi_2), \cdots, B^H(\varphi_n)\right),$$

*the Malliavin derivative of F is defined by*

$$D^H F = \sum_{i=1}^{n} \frac{\partial f}{\partial x_i}\left(B^H(\varphi_1), B^H(\varphi_2), \cdots, B^H(\varphi_n)\right)\varphi_i.$$

*The divergence operator $\delta^H$ is defined as the adjoint of $D^H$. For $u \in \mathrm{Dom}(\delta^H)$,*

$$\mathbb{E}[F\delta^H(u)] = \mathbb{E}\left[\left\langle D^H F, u\right\rangle_{\mathcal{H}}\right],$$

*where*

$$\delta^H(u) = \int_0^T u(s)\,\delta B^H(s).$$

*These definitions are used to characterize the stochastic integrals driven by fBm in the subsequent analysis.*

**Definition 3.** *The error trajectories $z_i(t)\,(i \in \mathbb{N})$ are mean-square exponential stability provided that constants $M > 0$ and $\mu > 0$, satisfying*

$$\mathbb{E}[\|z_i(t)\|]^2 \leq Me^{-\mu t},\ \forall t \geq 0, \tag{2.3}$$

*where the constant $\mu$ represents the exponential synchronization rate.*

## 3. Adaptive non-Markovian disturbance neural networks model

### *3.1. The adaptive non-Markovian perturbation model*

The following formulation introduces the adaptive non-Markovian perturbation model

$$dN_i(t) = \sigma_i(t, z_i(t))\Big(\int_0^t K(t,s)dB^H(s) + \Theta_i(t)\int_{t-\tau(t)}^t W(t,s)z_i(s)dsdB^1(t)\Big), \tag{3.1}$$

where $\sigma_i(t, z_i(t))$ denotes the intensity of the disturbance tied to the state, and $z_i(t)$ is the state vector, $K(t,s)$ is the memory kernels, $W(t,s)$ is the Gaussian weight function given in Assumption 5, $dB^H(s)$ and $dB^1(t)$ denote fractional and standard Brownian motion increments, respectively, $\Theta_i(t)$ is the adaptive switching function, and $\tau(t)$ is the time-varying delay.

**Remark 4.** *The time-varying adaptive coefficient $\Theta_i(t)$ regulates the contribution of the delayed history-dependent term $\int_{t-\tau(t)}^t W(t,s)z_i(s)\,ds$ to the Brownian perturbation of the ith node, thereby characterizing its time-varying sensitivity to disturbances from delayed states. Physically, $\Theta_i(t)$ acts as an amplification or attenuation factor reflecting variations in memory, delay, noise, or coupling effects; engineeringly, it corresponds to an adjustable noise gain or channel-uncertainty coefficient. Its introduction enables the disturbance model to capture unknown or time-varying perturbation effects beyond fixed constants. Accordingly, model (3.1) is termed an adaptive non-Markovian perturbation model, as it unifies the fBm-induced long-memory effect, the distributed-delay-induced history dependence, and the time-varying modulation by $\Theta_i(t)$.*

The specific expressions are given as follows:

$$\sigma_i(t, z_i(t)) = \sigma_0\Phi(\|z_i(t)\|)\Psi(t),$$

with $\sigma_0$ representing the baseline disturbance intensity.

The state-sensitive function

$$\Phi(\|z_i(t)\|) = \begin{cases} 1 + \aleph_1 e^{-\aleph_2 \|z_i(t)\|}, & \|z_i(t)\| \leq \hat{\delta}, \\ \aleph_3 \left(1 + \|z_i(t)\|\right)^{-\aleph_4}, & \|z_i(t)\| > \hat{\delta}, \end{cases}$$

where $\hat{\delta}$ denotes the threshold separating small and large deviation regimes. Parameters $\aleph_1, \aleph_2$ control the adjustment in the small-deviation regime, while $\aleph_3, \aleph_4$ govern the large-deviation regime. The time evolution function is given by

$$\Psi(t) = 1 + A\sin(\omega t + \varphi)e^{-\nu t},$$

where $A\sin(\omega t + \varphi)e^{-\nu t}$ represents an oscillatory attenuation term, $e$ represents the error that we will introduce it in the next section, and $\nu$ is the exponential decay rate. The memory kernel function $K(t, s)$ satisfies

$$K(t, s) = \begin{cases} 0, & \text{if } t \leq s, \\ \dfrac{(t-s)^{\alpha-1} e^{-\lambda(t-s)}}{\Gamma(\alpha)}, & \text{if } t > s, \end{cases} \tag{3.2}$$

where $\alpha \in (0, 1)$ controls the rate of memory decay, $\lambda > 0$ is the forgetting factor, and $s \in (0, t)$. The sigmoid adaptive switch $\Theta_i(t)$ is described by

$$\Theta_i(t) = \frac{1}{1 + e^{-\Delta(\vartheta_i(t) - \vartheta_{th})}},$$

where $\Delta > 0$ is the steepness parameter; $\vartheta_i(t)$ is the network status assessment. The network status assessment $\vartheta_i(t)$ is determined by $\vartheta_i(t) = \sum_{j\in\mathcal{N}_i} C_{ij} \left\| z_j(t) - z_i(t) \right\|^2$, where $\mathcal{N}_i$ denotes the neighborhood of node $i$ and $C_{ij}$ is the coupling weight between nodes $i$ and $j$, and $\vartheta_{th}$ is the switching threshold that satisfies the below conditions

$$\vartheta_i(t) \ll \vartheta_{th} \Rightarrow \Theta_i(t) \to 0\,(t \to \infty),$$
$$\vartheta_i(t) \gg \vartheta_{th} \Rightarrow \Theta_i(t) \to 1\,(t \to \infty).$$

### 3.2. System model

Based on the preliminaries above, the drive system takes the expression for a time-varying delayed neural network as follows

$$\begin{cases} dx_i(t) = [-A_1 x_i(t) + A_2 \hat{\eta}(x_i(t)) + A_3 \hat{\mu}(x_i(t - \tau(t))) + \tilde{B}]dt, \\ x_i(s) = \hat{\chi}_i(s), \ \ s \in [-\tau, 0], \end{cases} \tag{3.3}$$

where $x_i(t) = [x_1(t), x_2(t), \cdots, x_m(t)]^T \in \mathbb{R}^m$ stands for the state vector of the network. The matrix $A_1 = \mathrm{diag}\{a_1, a_2, \cdots, a_m\}$ represents the resistance parameter, with $a_i > 0$ for all $i = 1, 2, \cdots, m$, and is assumed to be diagonal. Matrices $A_2$ and $A_3$ correspond to the connection weights of neurons, while the neuron activation functions are expressed as $\hat{\eta}(x_i(t))$ and $\hat{\mu}(x_i(t - \tau(t)))$. The symbol $\tau(t)$ stands for the time varying delay satisfying $0 \leq \tau(t) \leq \tau$ and $\dot{\tau}(t) \leq \tilde{\tau} < 1$, where $\tilde{\tau}$ is a constant. The vector $\tilde{B} \in \mathbb{R}^m$ represents the external signal. System (3.3) is subjected to the initial condition $\hat{\chi}_i(s)$ $(i = 1, 2, \cdots, N)$.

**Remark 5.** *The existence of a constant $\tilde{\tau} > 0$ that binds the differential of the delay that varies with time function is a critical factor in studying exponential stability and synchronization in systems with time-varying delays. In most results [47, 49], $\tilde{\tau}$ is constrained to be less than 1 to facilitate Lyapunov-based stability analysis.*

We describe the response system by the following equations

$$\begin{cases} dy_i(t) = \Big[ - A_i y_i(t) + A_2\hat{\eta}(y_i(t)) + A_3\hat{\mu}(y_i(t-\tau(t))) + \tilde{B} + p\sum_{j=1}^{N} C_{ij}\left(y_j(t) - y_i(t)\right) + u_i(t)\Big]dt \\ \qquad\qquad +I_{M(t)}(E)\left(dN_i(t) + D_i(t)dB^2(t)\right), \\ I_{M(t)}(E) = \begin{cases} 1, & \text{if disturbance event } E \text{ occurs,} \\ 0, & \text{otherwise,} \end{cases} \\ y_i(s) = \chi_i(s),\ s \in [-\tau, 0], \end{cases} \tag{3.4}$$

where $y_i(t) = [y_1(t), y_2(t), \cdots, y_m(t)]^T \in \mathbb{R}^m$ is the response neuron behavior vector, representing the state of the corresponding $i$th response neural network; the parameter $p$ represents the strength of the coupling connecting the $j$th and $i$th nodes within the network, and the network's connectivity is encoded in the Laplacian matrix $C_L = (C_{ij})_{N\times N}$ derived from the adjacency matrix and representing the internal response structure; $I_{M(t)}(E)$ that indicates whether an event $E$ has occurred, which represents the occurrence of intermittent disturbances in the neural network and $M(t)$ is regarded as a Markov chain that undergoes random transitions between states, and event $E$ is triggered periodically based on the state transitions of $M(t)$; the term $u_i(t)$ represents the feedback control input; $dN_i(t)$ and $dB^2(t)$ denote the adaptive non-Markovian perturbation and the internal standard Brownian motion noise process, respectively; the initial conditions of system (3.4) are expressed as $\chi_i(\cdot)$, where $i \in 1, 2, \cdots, N$; and $\tau$ retains the same definition as in system (3.3).

$\{M(t), t \geq 0\}$ is a right-continuous homogeneous continuous-time Markov chain taking values in the finite mode set

$$\mathcal{S} = \{1, 2, \cdots, q\},$$

its transition probability satisfies

$$\Pr\{M(t+\Delta) = \ell \mid M(t) = r\} = \begin{cases} q_{r\ell}\Delta + o(\Delta), & r \neq \ell, \\ 1 + q_{rr}\Delta + o(\Delta), & r = \ell, \end{cases}$$

where $\Delta > 0$, $q_{r\ell} \geq 0$ for $r \neq \ell$, and

$$q_{rr} = -\sum_{\ell\neq r} q_{r\ell}.$$

The matrix

$$Q = (q_{r\ell})_{q\times q}$$

is called the transition-rate matrix of $M(t)$.

The evolution of the error dynamics in complex neural networks is expressed as

$$\begin{cases} dz_i(t) = \Big[-A_1 z_i(t) + A_2\eta_i(t) + A_3\mu_i(t) + p\sum_{j=1}^{N} C_{ij}\left(z_j(t) - z_i(t)\right) + u_i(t)\Big]dt \\ \qquad + I_{M(t)}(E)\left(dN_i(t) + D_i(t)dB^2(t)\right), \\ I_{M(t)}(E) = \begin{cases} 1, & \text{if disturbance event } E \text{ occurs,} \\ 0, & \text{otherwise,} \end{cases} \end{cases} \tag{3.5}$$

where $z_i(t) = y_i(t) - x_i(t)$ for $i \in \{1, 2, \cdots, N\}$ represents the error state trajectory, with $\eta_i(t) = \hat{\eta}_i(y_i(t)) - \hat{\eta}_i(x(t))$ and $\mu_i(t) = \hat{\mu}(y_i(t-\tau(t))) - \hat{\mu}(x_i(t-\tau(t)))$.

## 4. Main results

### *4.1. Controller design and adaptive law*

We design the controller as follows

$$u_i(t) = -k_i(t)z_i(t) - \gamma_i(t)\int_0^t K(t,s)z_i(s)ds + \beta\sum_{j=1}^{N} C_{ij}(z_j(t) - z_i(t)), \tag{4.1}$$

where $k_i(t)$ is the adaptive gain coefficient

$$k_i(t) = k_0 e^{\varrho\|z_i(t)\|^2},$$

with $k_0$ being the initial gain value (when $\|z_i(t)\| = 0$), and $\varrho$ controlling the gain sensitivity. $\gamma_i(t)$ denotes the intensity of the disturbance that depends on the state

$$\gamma_i(t) = \gamma_0\Phi(\|z_i\|)\Psi(t),$$

where $\gamma_0$ is the benchmark intensity of memory feedback. Parameter $\beta > 0$ represents the control gain corresponding to the interaction between $z_j(t)$ and $z_i(t)$ $(j \neq i)$.

The update laws for these parameters ($\aleph_i > 0$, $i \in \{1, 2, 3, 4\}$) depend on the performance index $J(t)$ defined as

$$J(t) = w_1\sum_{i=1}^{n}\|z_i(t)\|^2 + w_2\sum_{i=1}^{n}\|u_i(t)\|^2 + w_3\sum_{i=1}^{n}\int_{t-T}^{t}\left\|z_i(\hat{t})\right\|^2 d\hat{t},$$

where $T \in \mathbb{N}$, and $w_1$, $w_2$, $w_3$ represent the corresponding weighting coefficients.

The dynamic adjustment of controller parameters $k_0$ and $\gamma_0$ follows the gradient descent method

$$\frac{dk_0}{dt} = -\phi_6\frac{\partial J(t)}{\partial k_0}, \quad \frac{d\gamma_0}{dt} = -\phi_7\frac{\partial J(t)}{\partial\gamma_0}. \tag{4.2}$$

The state sensitive function parameter updates follow these update laws

$$\dot{\aleph}_1(t) = -\phi_1\frac{\partial J(t)}{\partial\aleph_1}, \quad \dot{\aleph}_2(t) = -\phi_2\frac{\partial J(t)}{\partial\aleph_2},$$

$$\dot{\aleph}_3(t) = -\phi_3 \frac{\partial J(t)}{\partial \aleph_3}, \quad \dot{\aleph}_4(t) = -\phi_4 \frac{\partial J(t)}{\partial \aleph_4}. \tag{4.3}$$

If we need to optimize fractional order noise modeling, the Hurst parameter $H$ can be synchronously adjusted by

$$\dot{H}(t) = -\phi_5 \frac{\partial J(t)}{\partial H}. \tag{4.4}$$

Note that $\phi_k > 0$ ($k \in \{1, 2, 3, 4, 5, 6, 7\}$) represent the learning rates.

*4.2. The main results*

**Theorem 1.** *If AssumptionS 1–5 hold, for constants $k_1, k_2, d, p$, and $\beta$, suppose that there exists $\mu > 0$ to satisfy the following condition*

$$\Lambda > 1, \quad \mu > \frac{\Lambda_5}{\Lambda - 1}, \tag{4.5}$$

*as a result, the error systems defined in* (3.5) *achieve mean-square exponential stability, which guarantees exponential synchronization of the response networks with the drive network.*

$$\Lambda = 2\Lambda_1 - 2\Lambda_2 k_1 - 2|d| k_2 \Lambda_3 + 2(p + \beta)\Lambda_4 - \gamma_{max},$$

*where*

$$\begin{aligned} \Lambda_1 &= \lambda_{\min}(A_1 + k_i(t) I_m), \quad \Lambda_2 = \lambda_{\max}(A_2), \\ \Lambda_3 &= \sqrt{\lambda_{\max}(A_3 A_3^T)}, \quad \Lambda_4 = \lambda_{min}(C_L), \\ \Lambda_5 &= \gamma_{max}\kappa_2 + \tau W_{\max}^2 + 2\kappa_1 \end{aligned} \tag{4.6}$$

*and $k_1, k_2$ denote positive constants introduced in* (2.1)*, the constant $d$ is introduced in the subsequent proof, parameter $p$ is specified as a constant in* (3.4)*, In* (4.1)*, $\beta$ is introduced as a strictly positive constant.*

*Proof.* With the controller (4.1) employed for the error system, system (3.5) can be recast as

$$\begin{aligned} dz_i(t) =& F(t)dt + I_{M(t)}(E)\sigma_i(t, z_i(t)) \int_0^t K(t, s) dB^H(s) \\ &+ I_{M(t)}(E)\Theta_i(t) \int_{t-\tau(t)}^t W(t, s) z_i(s) ds \cdot dB^1(t) + I_{M(t)}(E) D_i(t) dB^2(t), \end{aligned} \tag{4.7}$$

where the drift term $F(t)$ is expressed by

$$\begin{aligned} F(t) =& -\sum_{i=1}^{N} (A_1 + k_i(t) I_m) z_i(t) + A_2 \eta_i(t) + A_3 \mu_i(t) \\ &+ (p + \beta) \sum_{i=1}^{N} C_{ij} \left( z_j(t) - z_i(t) \right) - \gamma_i(t) \int_0^t K(t, s) z_i(s) ds, \end{aligned}$$

and $I_m$ is defined as an identity matrix of order $m$.

For stability analysis, we propose the following Lyapunov function

$$V = V_1 + V_2 + V_3,$$

where

$$V_1 = \frac{1}{2}\sum_{i=1}^{N} z_i^T(t)z_i(t),$$
$$V_2 = \frac{1}{2}\sum_{i=1}^{N}\int_{t-\tau(i)}^{t} z_i^T(s)z_i(s)ds,$$

and

$$V_3 = \sum_{i=1}^{N}\int_0^t\int_0^s K(s,u)z_i^T(u)z_i(u)du\,ds.$$

The first function $V_1(t)$ can be obtained by employing the fractional Itô's formulae as follows:

$$dV_1(t) = \sum_{i=1}^{N} z_i^T(t)dz_i(t) + \frac{1}{2}\sum_{i=1}^{N} dz_i^T(t)dz_i(t), \tag{4.8}$$

we can derive that

$$\begin{aligned} &dV_1(t)\\ =& -\sum_{i=1}^{N} z_i^T(t)\left(A_i + k_i(t)I_m\right)z_i(t)dt \ + \sum_{i=1}^{N} z_i^T(t)A_i\eta_i(t)dt\\ &+ (p+\beta)\sum_{i=1}^{N}\sum_{j=1}^{N} z_i^T(t)C_{ij}\Big(z_j(t) - z_i(t)\Big)dt + \sum_{i=1}^{N} D_i(t)dB^2(t)\\ &- \gamma_i(t)\sum_{i=1}^{N} z_i^T(t)\int_0^t K(t,s)z_i(s)ds\,dt + \sum_{i=1}^{N} z_i^T(t)A_i\mu_i(t)dt\\ &+ I_{M(t)}(E)z_i^T(t)\Big[\sum_{i=1}^{N}\sigma_i(t,z_i(t))\int_0^t K(t,s)dB^H(s)\\ &+ \Theta_i(t)\int_{t-\tau(t)}^{t} W(t,s)z_i(s)dsdB^1(t)\Big] + \frac{1}{2}I_{M(t)}^2(E)D_i^2(t)dt\\ &+ \frac{1}{2}\sum_{i=1}^{N} I_{M(t)}^2(E)\Theta_i^2(t)\int_{t-\tau(t)}^{t} W^2(t,s)z_i^2(s)dsdt\\ &+ \frac{1}{2}\sum_{i=1}^{N} I_{M(t)}^2(E)\sigma_i^2(t,z_i(t))(\int_0^t K(t,s)dB_H(s))^2dt, \end{aligned} \tag{4.9}$$

where

$$G_1 = -\sum_{i=1}^{N} z_i^T(t)(A_i + k_i(t)I_m)z_i(t),$$

$$
\begin{aligned}
G_2 &= \sum_{i=1}^{N} z_i^T(t)A_2\eta_i(t),\\
G_3 &= \sum_{i=1}^{N} z_i^T(t)A_3\mu_i(t),\\
G_4 &= (p+\beta)\sum_{i=1}^{N}\sum_{j=1}^{N} z_i^T(t)C_{ij}(z_j(t)-z_i(t)),\\
G_5 &= -\gamma_i(t)\sum_{i=1}^{N} z_i^T(t)\int_0^t K(t,s)z_i(s)ds,\\
G_6 &= \frac{1}{2}I_{M(t)}^2(E)D_i^2(t),\\
G_7 &= \frac{1}{2}I_{M(t)}^2(E)\Theta_i^2(t)\sum_{i=1}^{N}\int_{t-\tau(t)}^t W^2(t,s)z_i^2(s)ds,\\
G_8 &= \frac{1}{2}\sum_{i=1}^{N} I_{M(t)}^2(E)\sigma_i^2(t,z_i(t))(\int_0^t K(t,s)dB_H(s))^2,\\
G_9 &= I_{M(t)}(E)z_i^T(t)D_i(t)dB^2(t),\\
G_{10} &= I_{M(t)}(E)\sum_{i=1}^{N} z_i^T(t)\sigma_i(t,z_i(t))\int_0^t K(t,s)dB^H(s),
\end{aligned}
$$

and

$$
G_{11} = I_{M(t)}(E)z_i^T(t)\Theta_i(t)\int_{t-\tau(t)}^t W(t,s)z_i(s)ds\,dB^1(t).
$$

To derive the target outcomes, we implement the following mathematical approaches for (4.9)

$$
\begin{aligned}
G_1 &= -\sum_{i=1}^{N} z_i^T(t)(A_i + k_i(t)I_m)z_i(t)\\
&\leq -\lambda_{\min}(A_i + k_i(t)I_m)\sum_{i=1}^{N} z_i^T(t)z_i(t)\\
&= -2\Lambda_1 V_1(t).
\end{aligned}
\tag{4.10}
$$

Based on the inequalities given in Assumption 1, we can readily derive that

$$
(\xi_1-\xi_2)[(\check{\eta}(\xi_1)-\check{\eta}(\xi_2))-k_1(\xi_1-\xi_2)] \leq 0. \tag{4.11}
$$

From (4.11), we obtain the following inequality

$$
(y_i(t)-x_i(t))^T[(\check{\eta}(y_i(t))-\check{\eta}(x_i(t)))-k_1(y_i(t)-x_i(t)] \leq 0,
$$

leading to

$$
z_i^T(t)[(\eta_i(t)-k_1z_i(t)] \leq 0.
$$

This means that

$$z_i^T(t)\eta_i(t) \leq k_1 z_i^T(t) z_i(t),$$

so we can derive

$$\begin{aligned} G_2 &= \sum_{i=1}^{N} z_i^T(t) A_2 \eta_i(t) \\ &\leq \lambda_{\max}(A_2) k_1 \sum_{i=1}^{N} z_i^T(t) z_i(t) \\ &= 2\Lambda_2 k_1 V_1(t). \end{aligned} \tag{4.12}$$

Subsequently, we address $G_3$

$$\begin{aligned} G_3 &= \sum_{i=1}^{N} z_i^T(t) A_3 \mu_i(t) \\ &\leq \sum_{i=1}^{N} \sqrt{z_i(t) A_3 \mu_i(t) \mu_i^T(t) A_3^T z_i(t)} \\ &\leq \sqrt{\lambda_{\max}(A_3 A_3^T)} \sum_{i=1}^{N} \|z_i^T(t)\| \|\mu_i(t)\| \\ &= \Lambda_3 \sum_{i=1}^{N} \|z_i^T(t)\| \|\breve{\mu}(y_i(t-\tau(t))) - \breve{\mu}(x_i(t-\tau(t)))\| \\ &\leq k_2 \Lambda_3 \sum_{i=1}^{N} \|z_i^T(t)\| \|y_i(t-\tau(t)) - x_i(t-\tau(t))\| \\ &= |d| k_2 \Lambda_3 \sum_{i=1}^{N} \|z_i(t)\|^2 \\ &= 2|d| k_2 \Lambda_3 V_1(t). \end{aligned} \tag{4.13}$$

where $d$ is a constant arising from the time-delay state transformation inequality.

The network connectivity of the response–drive system is modeled as an undirected graph, where the coupling coefficients satisfy $C_{ij} = C_{ji}$ for all $i, j \in \mathbb{N}$.

Consequently, we can derive that

$$\begin{aligned} G_4 &= (p+\beta) \sum_{i=1}^{N} \sum_{j=1}^{N} z_i^T(t) C_{ij}(z_j(t) - z_i(t)) \\ &= (p+\beta) \sum_{i,j=1}^{N} C_{ij} z_i^T(t)(z_j(t) - z_i(t)) \\ &= -\frac{p+\beta}{2} \sum_{i,j=1}^{N} C_{ij}(z_j(t) - z_i(t))^T (z_j(t) - z_i(t)) \end{aligned}$$

$$= -(p+\beta)\sum_{i=1}^{N} z_i^T(t)C_L z_i(t)$$
$$\leq -2(p+\beta)\lambda_{min}(C_L)V_1(t), \tag{4.14}$$

where $C_L$ is a Laplacian matrix with all eigenvalues non-negative, and its smallest eigenvalue satisfies $\lambda_{min}(C_L) > 0$ .

Based on Assumptions 2 and 3 and by applying the Cauchy–Schwarz inequality, $G_5$ is derived

$$\begin{aligned}
G_5 &= -\gamma_i(t)\sum_{i=1}^{N}\int_0^t z_i^T(t)K(t,s)z_i(s)\,ds \\
&\leq \frac{1}{2}\gamma_{max}\sum_{i=1}^{N}\left(||z_i(t)||^2 + \int_0^t K^2(t,s)||z_i(s)||^2 ds\right) \\
&\leq \frac{1}{2}\gamma_{max}\sum_{i=1}^{N}\left(||z_i(t)||^2 + \kappa_2\int_0^t ||z_i(s)||^2 ds\right) \\
&= \gamma_{max}V_1(t) + \gamma_{max}\kappa_2\int_0^t V_1(s)ds,
\end{aligned} \tag{4.15}$$

where the memory kernel $K(t,s)$ is uniformly bounded.

Based on Assumption 4, we derive that

$$G_6 = \frac{1}{2}I^2_{M(t)}(E)D_i^2(t) \leq \frac{1}{2}D^2_{max}. \tag{4.16}$$

The term $G_7$ representing delayed coupling effects is bounded as, by Cauchy-Schwarz

$$\begin{aligned}
G_7 &= \frac{1}{2}\sum_{i=1}^{N} I^2_{M(t)}(E)\Theta_i^2(t)\int_{t-\tau(t)}^{t} W^2(t,s)z_i^2(s)ds \\
&\leq \frac{1}{2}\sum_{i=1}^{N}\tau(t)W^2_{\max}\int_{t-\tau(t)}^{t} z_i(s)^2\,ds \\
&\leq \tau W^2_{\max}\int_{t-\tau(t)}^{t} V_1(s)ds.
\end{aligned} \tag{4.17}$$

The stochastic term $G_8$ is bounded as follows

$$\begin{aligned}
G_8 &= \frac{1}{2}\sum_{i=1}^{N} I^2_{M(t)}(E)\sigma_i^2(t,z_i(t))(\int_0^t K(t,s)dB_H(s))^2 \\
&\leq \frac{1}{2}\sigma^2_{max}\sum_{i=1}^{N}\int_0^t\int_0^t K(t,s)K(t,s_1)\varphi_H(s,s_1)dsds_1,
\end{aligned}$$

and the function $\iota_H(t,s)$ is

$$\iota_H(t,s) = H(2H-1)|t-s|^{2H-2}, \tag{4.18}$$

through substitution $r_1 = t - s$, $r_2 = t - s_1$, from (3.2) and (4.18)

$$\begin{aligned}
&\int_0^t K(t,s)K(t,s_1)\varphi_H(s,s_1)dsds_1\\
=&\frac{H(2H-1)}{\Gamma(\alpha)^2}\int_0^t\int_0^t r_1^{\alpha-1}r_2^{\alpha-1}e^{-\lambda(r_1+r_2)}|r_1-r_2|^{2H-2}dr_1dr_2\\
\leq&\frac{H(2H-1)}{\Gamma(\alpha)^2}\int_0^\infty\int_0^\infty r_1^{\alpha-1}r_2^{\alpha-1}e^{-\lambda(r_1+r_2)}|r_1-r_2|^{2H-2}dr_1dr_2\\
:=&C_H.
\end{aligned}$$

By Assumption 3, the right-hand double integral converges and is a finite constant. Thus, we obtain the final bound

$$G_8 \leq \frac{1}{2}\sigma_{max}^2\sum_{i=1}^N C_H \leq \frac{N}{2}\sigma_{max}^2 C_H. \tag{4.19}$$

Combining the estimation results (4.10), (4.12)–(4.17), (4.19), the martingale property of Brownian motion, and the zero-mean property of the fBm term, there are $\mathbb{E}[dB_H(s)] = 0$, $\mathbb{E}[dB^1(t)] = 0$, and $\mathbb{E}[dB^2(t)] = 0$. We derive this inequality

$$\begin{aligned}
&\mathbb{E}[dV_1(t)]\\
\leq&-2\Lambda_1\mathbb{E}[V_1(t)]dt + 2\Lambda_2 k_1\mathbb{E}[V_1(t)]dt\\
&+2|d|k_2\Lambda_3\mathbb{E}[V_1(t)]dt - 2(p+\beta)\Lambda_4\mathbb{E}[V_1(t)]dt\\
&+\gamma_{max}\mathbb{E}[V_1(t)]dt + \gamma_{max}\kappa_2\mathbb{E}\left(\int_0^t V_1(s)dsdt\right)\\
&+\tau_{\max}W_{\max}^2\mathbb{E}\left(\int_{t-\tau(t)}^t V_1(s)ds\right)dt + \mathbb{E}[\overline{C}]dt,
\end{aligned}$$

where the combined constant term is

$$\overline{C} = \frac{N}{2}\sigma_{max}^2 C_H + \frac{1}{2}D_{\max}^2.$$

Considering that

$$\int_{t-\tau(t)}^t V_1(s)ds \leq \int_0^t V_1(s)ds,$$

we obtain the simplified form

$$\mathbb{E}[dV_1(t)] \leq -\Lambda\mathbb{E}[V_1(t)]dt + (\gamma_{max}\kappa_2 + \tau W_{\max}^2)\int_0^t \mathbb{E}\left[V_1(s)\right]dsdt + \overline{C}dt. \tag{4.20}$$

The time-delay term evolves as

$$\begin{aligned}
&\mathbb{E}[dV_2(t)]\\
=&\mathbb{E}\left[\frac{d}{dt}\left(\frac{1}{2}\sum_{i=1}^N\int_{t-\tau(t)}^t z_i^T(s)z_i(s)ds\right)\right]dt
\end{aligned}$$

$$
\begin{aligned}
&=\frac{1}{2}\mathbb{E}\left[\sum_{i=1}^{N}\|z_i(t)\|^2-(1-\dot{\tau}(t))\sum_{i=1}^{N}\|z_i(t-\tau(t))\|^2\right]dt\\
&\leq\mathbb{E}[V_1(t)]dt. \qquad (4.21)
\end{aligned}
$$

The evolution of the distributed memory term $V_3(t)$ is expressed as

$$
dV_3(t)=\frac{d}{dt}\left[\sum_{i=1}^{N}\int_0^t(\int_0^s K(s,r)z_i^T(r)z_i(r)\,dr)ds\right]dt,
$$

and by exchanging the order of integration (Fubini's theorem), the integration region $0\leq r\leq s\leq t$ can be rewritten for iterated integration as $\int_{r=0}^{t}\int_{s=r}^{t}\cdots\,ds\,dr$, so we have

$$
\begin{aligned}
\mathbb{E}[dV_3(t)]&=\mathbb{E}\left[\frac{d}{dt}\sum_{i=1}^{N}\int_0^t\left(\int_u^t K(s,r)\,ds\right)\|z_i(r)\|^2du\right]dt\\
&=\mathbb{E}\left[\sum_{i=1}^{N}\int_0^t K(t,r)z_i^T(r)z_i(r)du\right]dt\\
&\leq\kappa_1\mathbb{E}\left[\sum_{i=1}^{N}\int_0^t\|z_i(r)\|^2dr\right]dt\\
&=2\kappa_1\int_0^t\mathbb{E}[V_1(r)]drdt\\
&=2\kappa_1\int_0^t\mathbb{E}[V_1(s)]dsdt. \qquad (4.22)
\end{aligned}
$$

The total expected Lyapunov functional evolution combines all components

$$
\mathbb{E}[dV(t)]=\mathbb{E}[dV_1(t)]+\mathbb{E}[dV_2(t)]+\mathbb{E}[dV_3(t)]. \qquad (4.23)
$$

Substituting (4.20)–(4.22) into (4.23), we get

$$
\begin{aligned}
&\mathbb{E}[dV(t)]\\
&\leq-(\Lambda-1)\mathbb{E}[V(t)]dt+(\gamma_{max}\kappa_2\\
&\quad+\tau W_{\max}^2+2\kappa_1)\int_0^t\mathbb{E}\left[V(s)\right]dsdt+\overline{C}dt\\
&=-(\Lambda-1)\mathbb{E}[V(t)]dt+\Lambda_5\int_0^t\mathbb{E}\left[V(s)\right]dsdt+\overline{C}dt.
\end{aligned}
$$

Dividing both sides by $dt$ yields a differential inequality

$$
\frac{d}{dt}\mathbb{E}[V(t)]\leq-(\Lambda-1)\,\mathbb{E}[V(t)]+\Lambda_5\int_0^t\mathbb{E}[V(s)]ds+\overline{C}. \qquad (4.24)
$$

To handle the convolution term on the right of (4.24), let $\mu>0$ and define

$$
Q(t):=\sup_{0\leq s\leq t}e^{\mu s}\mathbb{E}[V(s)],
$$

(4.24) is multiplied by $e^{\mu t}$, producing

$$\frac{d}{dt}\left(e^{\mu t}\mathbb{E}[V(t)]\right)+(\Lambda-1-\mu)\,e^{\mu t}\mathbb{E}[V(t)]\leq\Lambda_5 e^{\mu t}\int_0^t\mathbb{E}[V(s)]ds+\overline{C}e^{\mu t}. \tag{4.25}$$

For the convolution term, note that for $0\leq s\leq t$, $\mathbb{E}[V(s)]\leq e^{-\mu s}Q(t)$,

$$\int_0^t\mathbb{E}[V(s)]ds\leq Q(t)\int_0^t e^{-\mu s}ds\leq\frac{Q(t)}{\mu}.$$

Thus, (4.25) can be reformulated as

$$\frac{d}{dt}\left(e^{\mu t}\mathbb{E}[V(t)]\right)+(\Lambda-1-\mu)\,e^{\mu t}\mathbb{E}[V(t)]\leq\frac{\Lambda_5}{\mu}e^{\mu t}Q(t)+\overline{C}e^{\mu t}.$$

Then, we set up $\Xi(t)=e^{\mu t}E[V(t)]$, and we can get

$$\Xi'(t)+(\Lambda-1-\mu)\,\Xi(t)\leq\frac{\Lambda_5}{\mu}e^{\mu t}Q(t)+\overline{C}e^{\mu t}. \tag{4.26}$$

Let the integration factor be

$$\epsilon(t)=e^{(\Lambda-1-\mu)t},$$

and multiplying both sides of (4.26) by $\epsilon(t)$, we get

$$\epsilon(t)\Xi'(t)+(\Lambda-1-\mu)\,\epsilon(t)\Xi(t)\leq\left(\frac{\Lambda_5}{\mu}Q(t)+\overline{C}\right)e^{\mu t}\epsilon(t),$$

then

$$\frac{d}{dt}(\epsilon(t)\Xi(t))\leq\left(\frac{\Lambda_5}{\mu}Q(t)+\overline{C}\right)e^{(\Lambda-1)t}.$$

Integrate the above formula from 0 to $t$

$$\epsilon(t)\Xi(t)-\Xi(0)\leq\int_0^t\left(\frac{\Lambda_5}{\mu}\epsilon(s)+\overline{C}\right)e^{(\Lambda-1)s}ds.$$

Thus

$$\Xi(t)\leq\Xi(0)e^{-(\Lambda-1-\mu)t}+e^{-(\Lambda-1-\mu)t}\int_0^t\left(\frac{\Lambda_5}{\mu}\epsilon(s)+\overline{C}\right)e^{(\Lambda-1)s}ds, \tag{4.27}$$

and $Q(t)$ is a monotonic non decreasing function, which can be further scaled

$$\int_0^t\epsilon(s)e^{(\Lambda-1)s}ds\leq Q(t)\int_0^t e^{(\Lambda-1)s}ds=Q(t)\frac{e^{(\Lambda-1)t}-1}{\Lambda-1}. \tag{4.28}$$

By substituting (4.28) into (4.27), we derive that

$$\Xi(t)\leq\Xi(0)e^{-(\Lambda-1-\mu)t}+Q(t)\frac{\Lambda_5}{\mu(\Lambda-1)}\left(1-e^{-(\Lambda-1)t}\right)+\frac{\overline{C}}{\Lambda-1}\left(1-e^{-(\Lambda-1)t}\right),$$

and we take the supremum for $t$

$$Q(t)\left(1-\frac{\Lambda_5}{\mu\,(\Lambda-1)}\right)\leq \Xi(0)+\frac{\overline{C}}{\Lambda-1}.$$

To ensure that $Q(t)$ is bounded, it is necessary to let

$$1-\frac{\Lambda_5}{\mu\,(\Lambda-1)}>0.$$

Thus,

$$Q(t)\leq \frac{\Xi(0)+\frac{\overline{C}}{\Lambda-1}}{1-\frac{\Lambda_5}{\mu(\Lambda-1)}}.$$

Since $\Xi(t)=e^{\mu t}E[V(t)]\leq Q(t)$, therefore

$$\mathbb{E}[V(t)]\leq Q(t)e^{-\mu t}\leq \left(\frac{\mathbb{E}[V(0)]+\frac{\overline{C}}{\Lambda-1}}{1-\frac{\Lambda_5}{\mu(\Lambda-1)}}\right)e^{-\mu t}. \tag{4.29}$$

Moreover, $\Lambda>1$ and $\mu>\frac{\Lambda_5}{\Lambda-1}$ from (4.5) and (4.29). Thus, in accordance with Definition 3, system (3.5) is exponentially mean-square stable. This establishes the desired result and concludes the proof. □

**Remark 6.** *The introduction of fBm, memory effects, intermittent disturbances, and time-varying delays improves the modeling ability of the proposed system, and increases its complexity. In particular, the memory term requires historical state information and thus increases the computational and storage costs. Moreover, the analysis is based on the parameter assumptions given in this paper. In practical systems, uncertainties may exist in connection weights, coupling parameters, time delays, and disturbance intensities, which may affect the synchronization performance. The treatment of parameter uncertainties and the reduction of model complexity will be considered in future work.*

**Remark 7.** *The Lyapunov functional is composed of three parts: $V_1(t)$ captures the instantaneous state energy, $V_2(t)$ accounts for the influence of time-varying delays, and $V_3(t)$ reflects the distributed memory effects induced by the non-Markovian disturbance model. This construction ensures that all the characteristics of the system, including the current state, delay, and memory, are considered simultaneously in the stability analysis. Such a design is crucial for systems with short-term and long-term dependencies, as neglecting any of these components may lead to overly conservative or invalid stability conditions.*

**Remark 8.** *It is worth noting that the final synchronization criterion does not explicitly depend on the intermittent switching parameters. This indicates that the proposed adaptive synchronization framework is robust with respect to admissible intermittent scheduling. From the practical viewpoint, the intermittent mechanism mainly serves to reduce controller activation time, communication frequency, and energy consumption. Therefore, although the switching parameters are absent from the final sufficient condition, the intermittent control strategy provides important implementation advantages over continuous control.*

**Remark 9.** *The differential $dV_1(t)$ in (4.8) is derived using a version of the Itô formula valid for integrals with respect to fBm. The second term, $\sum_{i=1}^{N} dz_i^T(t)dz_i(t)$, implicitly involves the Malliavin derivative and the covariance of fBm due to the expression $(dB_H(t))^2 = H(2H-1)|t-s|^{2H-2}ds$, which reflects the long-memory property of fBm. This quadratic variation-like term arises from the non-vanishing covariance structure of fBm increments and must be rigorously justified using the tools of fractional calculus. This distinguishes the analysis sharply from the case where $H = \frac{1}{2}$ (standard Brownian motion), where $(dB_{1/2}(t))^2 = dt$ due to the independent increments of the Wiener process. This distinction highlights the fundamental differences in the stochastic calculus of fBm. It also requires the use of specialized analytical tools such as Malliavin calculus and functional analysis techniques.*

## 5. Numerical simulations

To verify the theoretical results and evaluate the performance of the proposed adaptive memory controller, numerical simulations are conducted under adaptive non-Markovian stochastic perturbations. The simulations focus on three aspects: synchronization performance, comparison with conventional controllers, and scalability with respect to the network size.

### *5.1. Simulation setup*

The adaptive non-Markovian perturbation follows the state-dependent disturbance model introduced in Section 3. The relevant parameters are selected as $\sigma_0 = 0.04, \delta = 0.1, H = 0.7, \alpha_p = 0.5$, and $\lambda_p = 1.2$, and the corresponding memory integral is approximated using the most recent 50 sampling steps. $k_i(0) = 3.2, \gamma_i(0) = 1.6$, while the coupling gain is chosen as $\beta = 0.75$. The weighting coefficients in the performance index are selected as $\omega_1 = 1.5, \omega_2 = 0.02, \omega_3 = 0.03$, and the adaptive learning rates are $\phi_6 = 0.55, \phi_7 = 0.40, \eta_k = 1.6, \eta_\gamma = 1.0$. To guarantee numerical stability, the adaptive gains satisfy $1 \leq k_i(t) \leq 12, 0.4 \leq \gamma_i(t) \leq 8$. The controller memory kernel adopts $\alpha_c = 0.55, \lambda_c = 0.45$.

Consequences of Theorem 1: The parameters $\Lambda$, $\Lambda_1$, $\Lambda_2$, $\Lambda_3$, $\Lambda_4$, $\Lambda_5$, and $\mu$ are readily computed following the definitions provided

$$\Lambda = 2.802, \Lambda_1 = 4.117, \Lambda_2 = 0.4280,$$
$$\Lambda_3 = 0.3567, \Lambda_4 = 0, \Lambda_5 = 4.5, \mu = 2.5,$$

we can find that $\Lambda > 1$ and $\mu > \frac{\Lambda_5}{\Lambda - 1}$, thus complying with Theorem 1.

### *5.2. Synchronization performance*

Figures 1 and 2 show the synchronization trajectories of the first and second state components, respectively. Owing to different initial conditions and non-Markovian stochastic perturbations, noticeable state deviations appear at the beginning of the simulation. Under the proposed adaptive memory controller, all response states gradually converge to the corresponding drive states. This result demonstrates that the adaptive feedback and memory compensation mechanisms effectively suppress the disturbance and agrees well with the theoretical result in Theorem 1.

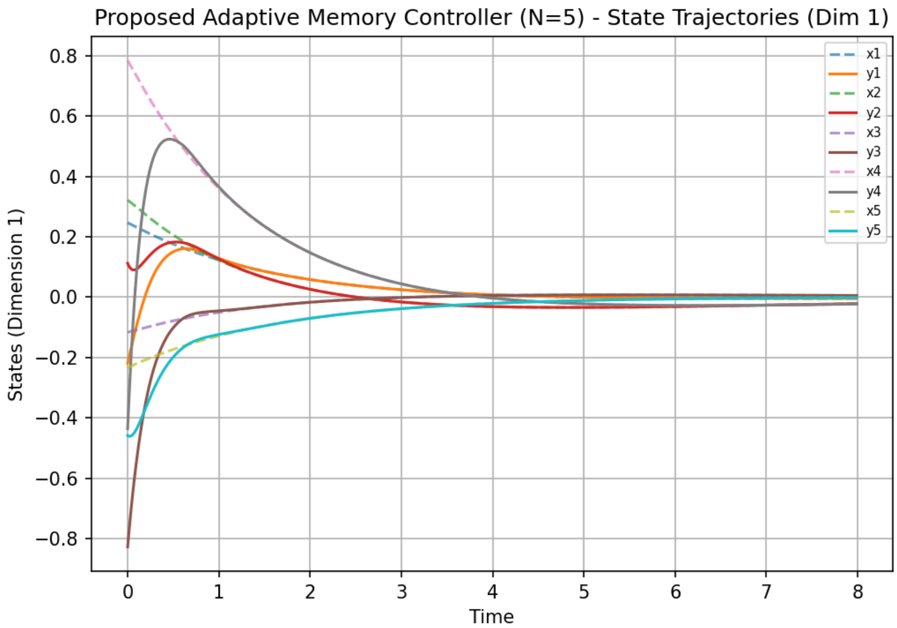


**Figure 1.** The state trajectories of the first dimension for each node under the proposed adaptive memory controller with N=5.

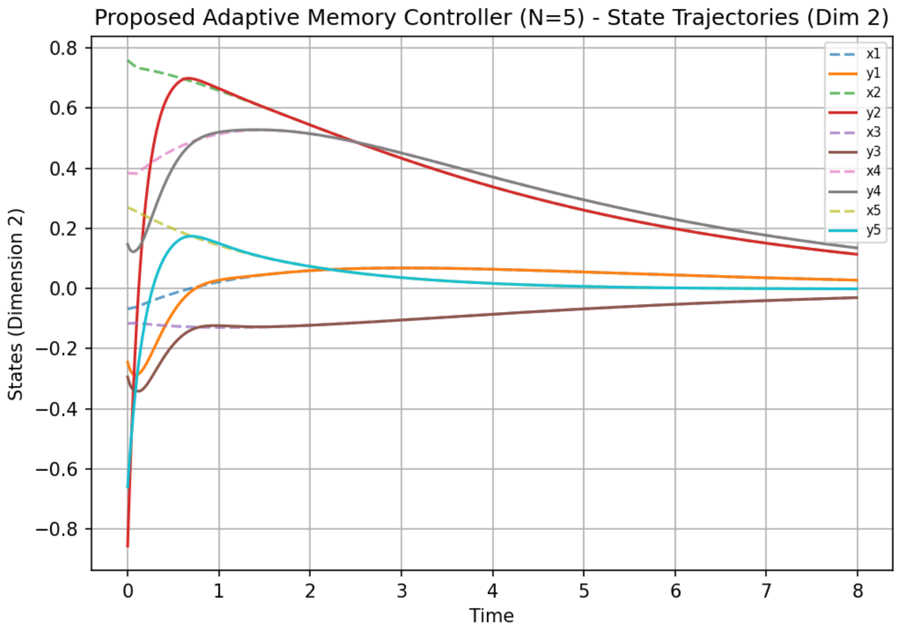


**Figure 2.** The state trajectories of the second dimension for each node under the proposed adaptive memory controller with N=5.

Figure 3 illustrates the control inputs generated by the proposed controller. Large control efforts are produced during the initial stage to rapidly reduce the synchronization errors, while the control inputs gradually approach zero as synchronization is achieved. This indicates that the adaptive mechanism can automatically adjust the control strength according to the synchronization errors.

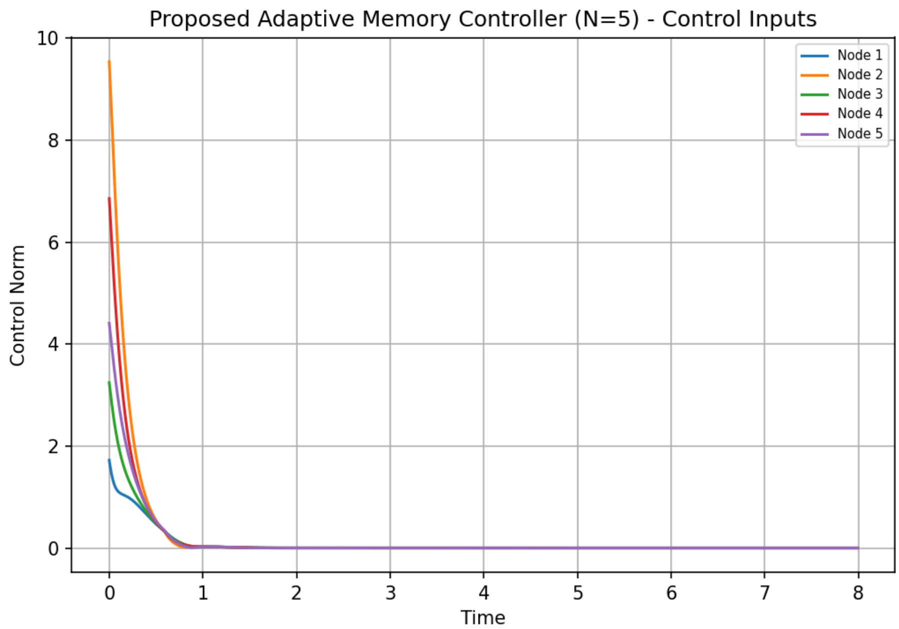


**Figure 3.** The Control input norms $\|u_i(t)\|$ for each node under the proposed adaptive memory controller with $N = 5$.

Figure 4 presents the overall synchronization error of the coupled neural network. The synchronization error decreases rapidly and converges to zero within a short time despite the presence of non-Markovian stochastic perturbations. The result verifies the effectiveness of the proposed controller and is consistent with the theoretical stability analysis. Figure 5 shows the evolution of the average synchronization error. The error decreases monotonically and remains close to zero after convergence, indicating that the proposed controller achieves stable synchronization for the network. This behavior further confirms the effectiveness of the adaptive memory compensation strategy.

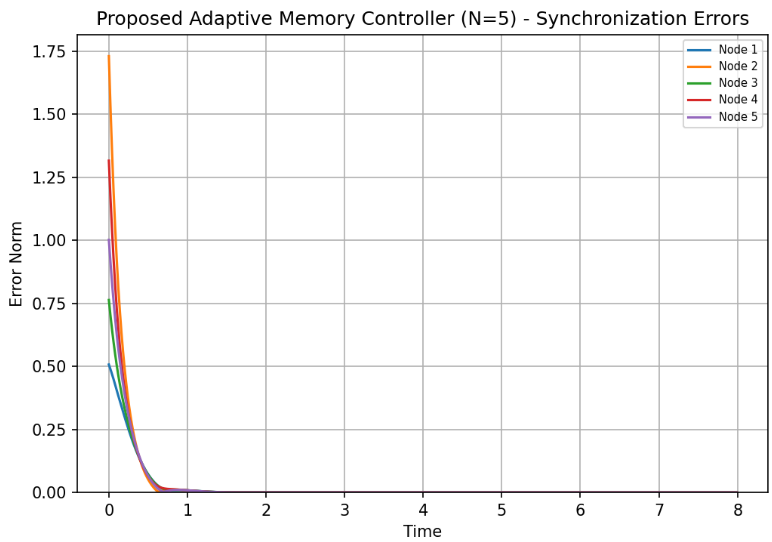


**Figure 4.** The Synchronization errors for each node under the proposed adaptive memory controller with $N = 5$.

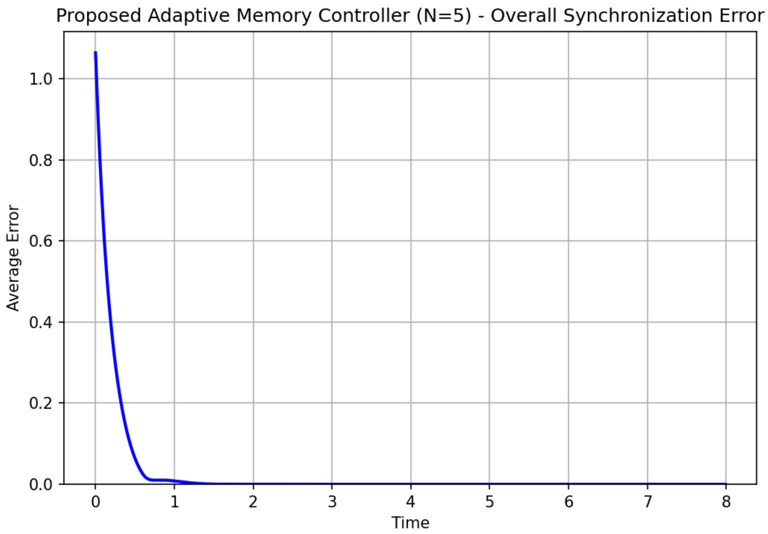


**Figure 5.** The overall synchronization error $||z_i(t)||^2$ for each node under the proposed adaptive memory controller with $N = 5$.

Figure 6 depicts the phase trajectories of the synchronization error system. All trajectories gradually converge toward the equilibrium point without divergence, demonstrating the stability of the closed-loop system. The phase portrait further validates the synchronization criterion established in Theorem 1.

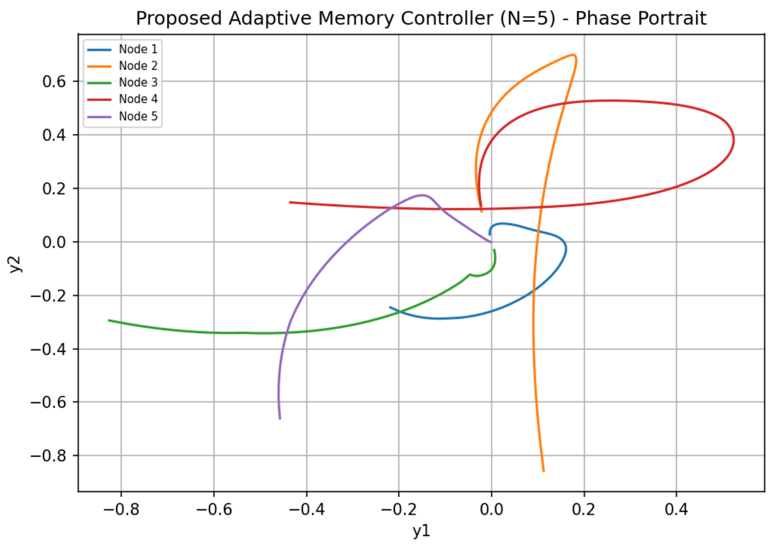


**Figure 6.** The state-space phase portrait of $z_1 - z_2$ for each node under the proposed adaptive memory controller with $N = 5$.

*5.3. Comparison with conventional controllers*

To further validate the effectiveness of the proposed adaptive memory controller, three widely used conventional controllers are adopted for comparison, namely, the linear feedback controller (LFC) [50], proportional-derivative (PD) controller [51], and proportional-integral-derivative (PID) controller [52]. All controllers are tested under identical network topology, initial conditions, neural-network parameters, and non-Markovian stochastic disturbances, with their parameters selected under the same conditions to ensure a fair comparison.

The LFC is implemented as

$$u_i(t) = -Kz_i(t) + \beta \sum_{j=1}^{N} A_{ij}(z_j(t) - z_i(t)),$$

with $K = 1.0$ and $\beta = 0.3$.

The PD controller is given by

$$u_i(t) = -K_p z_i(t) - K_d \dot{z}_i(t) + \beta \sum_{j=1}^{N} A_{ij}(z_j(t) - z_i(t)),$$

where $K_p = 1.2$, $K_d = 0.4$, and $\beta = 0.3$.

The PID controller is expressed as

$$u_i(t) = -K_p z_i(t) - K_i \int_0^t z_i(s)\,ds - K_d \dot{z}_i(t) + \beta \sum_{j=1}^{N} A_{ij}(z_j(t) - z_i(t)),$$

where $K_p = 1.0$, $K_i = 0.3$, $K_d = 0.35$, and $\beta = 0.3$.

We obtain the following simulation results: Figure 7 compares the synchronization errors of different controllers. The proposed adaptive memory controller exhibits the fastest convergence and reaches the synchronization state within approximately $0.91s$. In contrast, the LFC and PD controllers converge more slowly, while the PID controller exhibits obvious residual synchronization errors during the transient process. These results indicate that the adaptive gain adjustment together with the memory compensation mechanism effectively accelerates the synchronization process and suppresses adaptive non-Markovian stochastic perturbations.

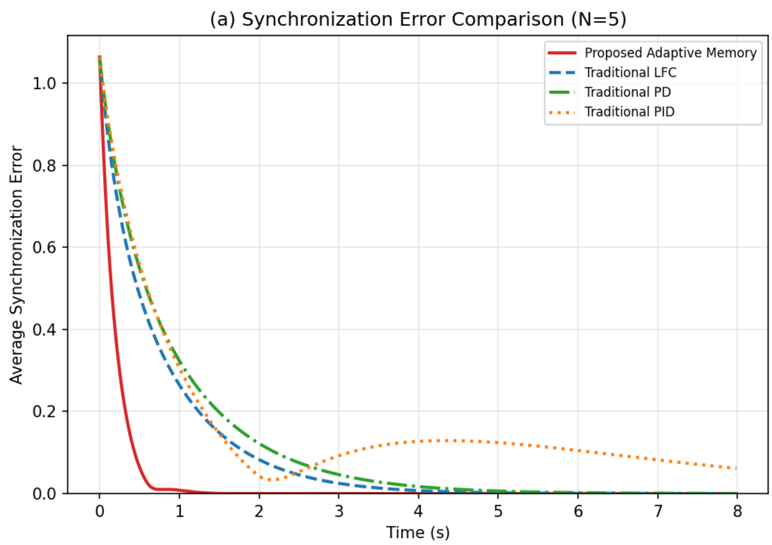


**Figure 7.** Comparison of synchronization errors under different controllers.

Figure 8 presents the control effort generated by different controllers. The proposed controller initially applies a relatively larger control input to rapidly eliminate the synchronization error and then quickly reduces the control effort after synchronization is achieved. This behavior demonstrates that the adaptive mechanism automatically allocates the control strength according to the synchronization error, leading to efficient synchronization without excessive control actions during the steady-state stage.

Figure 9 compares the quantitative synchronization performance in terms of Integral Square Error (ISE), Integral Absolute Error (IAE), and Integral Time Absolute Error (ITAE) values. The proposed adaptive memory controller achieves the smallest values for all three performance indices, indicating superior transient synchronization performance and higher synchronization accuracy. In particular, the significant reduction of ITAE demonstrates that the proposed controller effectively suppresses synchronization errors throughout the aevolution.

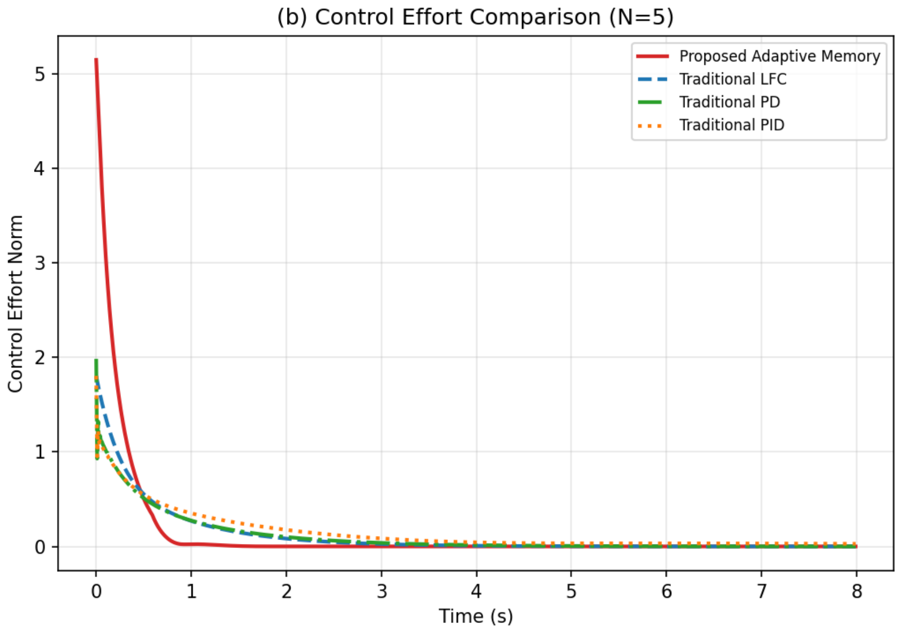


**Figure 8.** Comparison of control efforts under different controllers.

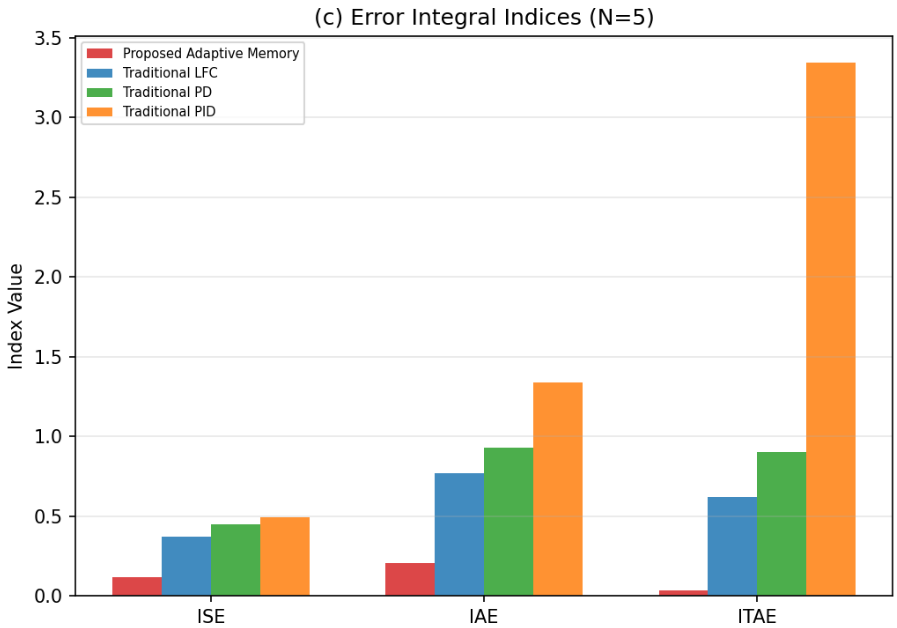


**Figure 9.** Comparison of error integral performance indices.

As shown in Table 2, the proposed adaptive memory controller achieves the smallest ISE, IAE, and ITAE among all compared methods. Moreover, it reaches synchronization within 0.91$s$, which is significantly faster than the LFC, PD, and PID controllers. These results demonstrate that the proposed controller provides faster convergence and higher synchronization accuracy under non-Markovian stochastic perturbations.

**Table 2.** Performance comparison of different controllers for $N = 5$.

| Controller | ISE | IAE | ITAE | Final Err | Settle(s) | Reduce(%) |
|---|---|---|---|---|---|---|
| **Proposed** | **0.1161** | **0.2067** | **0.0368** | **0** | **0.910** | **100** |
| LFC | 0.3711 | 0.7684 | 0.6222 | $8.2 \times 10^{-5}$ | 3.750 | 99.99 |
| PD | 0.4519 | 0.9289 | 0.9044 | $4.6 \times 10^{-4}$ | 4.550 | 99.96 |
| PID | 0.4958 | 1.3364 | 3.3453 | 0.0693 | 7.990 | 93.48 |

**Remark 10.** *The improved synchronization performance can be mainly attributed to the combined effects of adaptive gain adjustment and memory compensation. The adaptive mechanism dynamically adjusts the control gains according to the synchronization errors, while the memory term utilizes historical state information to compensate for the long-memory effects of the non-Markovian perturbations.*

As shown in Table 3, the proposed controller still achieves rapid synchronization when the network size is increased from $N = 5$ to $N = 15$. The synchronization errors converge to values close to zero, indicating that the proposed control strategy remains effective for the larger network considered in this simulation. These results further demonstrate the scalability of the proposed method under adaptive non-Markovian stochastic perturbations.

**Table 3.** Performance summary: N=5 and N=15.

| $N$ | Controller | ISE | IAE | ITAE | Final Err | RMS Err | Settle(s) | Ctrl Energy | Reduce(%) |
|---|---|---|---|---|---|---|---|---|---|
| 5 | **Proposed** | **0.1161** | **0.2067** | **0.0368** | **0** | **0.1205** | **0.910** | 2.8109 | **100.00** |
| 5 | LFC | 0.3711 | 0.7684 | 0.6222 | $8.16 \times 10^{-5}$ | 0.2154 | 3.750 | 0.6995 | 99.99 |
| 5 | PD | 0.4519 | 0.9289 | 0.9044 | $4.57 \times 10^{-4}$ | 0.2377 | 4.550 | 0.4841 | 99.96 |
| 5 | PID | 0.4958 | 1.3364 | 3.3453 | $6.93 \times 10^{-2}$ | 0.2489 | 7.990 | 0.5475 | 93.48 |
| 15 | **Proposed** | **0.0218** | **0.0545** | **0.0043** | **0** | **0.0522** | **0.370** | 4.6206 | **100.00** |
| 15 | LFC | 0.0531 | 0.1513 | 0.0485 | $4.39 \times 10^{-6}$ | 0.0815 | 1.330 | 1.5664 | 100.00 |
| 15 | PD | 0.0705 | 0.1994 | 0.0774 | $2.48 \times 10^{-5}$ | 0.0939 | 1.610 | 1.1256 | 100.00 |
| 15 | PID | 0.0701 | 0.2418 | 0.3183 | $7.36 \times 10^{-3}$ | 0.0936 | 4.830 | 1.1376 | 99.05 |

### *5.4. Discussion*

The above numerical results demonstrate that the proposed adaptive memory controller can effectively achieve synchronization under adaptive non-Markovian stochastic perturbations. In particular, the synchronization errors converge rapidly to zero, and satisfactory synchronization performance is maintained when the network size is increased from $N = 5$ to $N = 15$. These results indicate that the proposed method is effective for small- and relatively large-scale coupled neural networks.

The improved synchronization performance mainly results from the combination of adaptive feedback and memory compensation. The adaptive mechanism dynamically adjusts the controller gains according to the synchronization errors, providing sufficient control action when the errors are large. Moreover, the memory term incorporates historical state information and compensates for the long-memory effect of the non-Markovian perturbations. Therefore, the influence of state-dependent and history-dependent disturbances can be effectively attenuated.

The comparison with the LFC, PD, and PID controllers further supports this observation. The proposed method achieves smaller ISE, IAE, and ITAE values and a shorter settling time. Unlike conventional fixed-gain controllers, the proposed controller simultaneously adapts the feedback strength and compensates for the memory effect of the disturbances, which explains its faster convergence and higher synchronization accuracy.

Furthermore, the numerical observations are consistent with the theoretical results established in Theorem 1. The convergence of the synchronization errors toward zero and the bounded control inputs support the Lyapunov-based stability analysis. Hence, the simulations not only demonstrate the effectiveness of the proposed controller but also provide numerical verification of the derived synchronization criterion.

## 6. Conclusions

In this paper, we investigated the synchronization of coupled neural networks under adaptive non-Markovian stochastic perturbations and developed an adaptive memory controller. The theoretical analysis established sufficient synchronization conditions based on the Lyapunov functional method.

Several findings were obtained from the numerical simulations. First, the proposed controller drives the synchronization errors to zero and maintains bounded control inputs under non-Markovian stochastic perturbations. Second, satisfactory synchronization is achieved for $N = 5$ and $N = 15$, indicating that the proposed method remains effective as the network size increases. Third, compared with the conventional LFC, PD, and PID controllers, the proposed method achieves smaller ISE, IAE, and ITAE values. In particular, its settling time is $0.91s$, compared with $3.75s$, $4.55s$, and $7.99s$ for the LFC, PD, and PID controllers, respectively. These results show that the adaptive gain adjustment and memory compensation mechanisms improve convergence speed and synchronization accuracy.

Some limitations remain in this work. The derived stability conditions may be conservative due to the inequality estimates used in the Lyapunov analysis. Moreover, the adaptive gain updating and memory-kernel computation increase the computational complexity of the controller. The theoretical results also rely on assumptions such as the Lipschitz continuity of the activation functions.

In future research, we will focus on reducing the conservativeness of the derived synchronization conditions. Studies have shown that non-decomposition techniques can provide more relaxed synchronization criteria for fractional-order neural networks [53]. Therefore, extending such techniques to coupled neural networks under non-Markovian disturbances is an interesting direction for future research. Another possible direction is to improve the selection of controller parameters. Optimization methods based on quadratic inequalities and particle swarm optimization have been applied to obtain relaxed synchronization criteria [54]. Such optimization techniques may be incorporated into the proposed framework to optimize controller parameters and reduce the dependence on manually selected gains.

## Author contributions

Zixin Zhu: Conceptualization, Methodology, Visualization, Writing—original draft; Weihua Wan: Writing—review and editing, Supervision, Validation; Yuming Feng: Writing—original draft, Writing—review and editing, supervision; Xiangguang Dai: Writing—review and editing, Supervision, Validation. All authors have read and agreed to the published version of the manuscript.

## Use of Generative-AI tools declaration

The authors declare they have not used Artificial Intelligence (AI) tools in the creation of this article.

## Acknowledgments

This research is supported by the Science and Technology Research Program of Chongqing Municipal Education Commission (Grant Nos. KJQN202501242, KJQN202201221 ) and the Chongqing Natural Science Foundation (Grant Nos. CSTB2024NSCQ-LZX0083, CSTB2024NSCQ-LZX0119 ).

## Conflict of interest

The authors declare that they have no competing interests.

## References


1. G. Chen, J. Xia, J. H. Park, H. Shen, G. Zhuang, Sampled-data synchronization of stochastic Markovian jump neural networks with time-varying delay, *IEEE Trans. Neur. Net. Lear.*, **33** (2022), 3829–3841. https://doi.org/10.1109/TNNLS.2021.3054615
2. G. Chen, Optimal synchronization of higher-order dynamical networks, *Artificial Intelligence Science and Engineering*, **1** (2025), 31–36. https://doi.org/10.23919/AISE.2025.000003
3. T. Shi, C. Hu, J. Yu, Fixed-time synchronization of spatiotemporal networks via quantized boundary control, *Intelligence & Control*, **1** (2025), 3. https://doi.org/10.53941/ic.2025.100003
4. Y. Zhong, D. Song, Nonfragile synchronization control of T-S fuzzy Markovian jump complex dynamical networks, *Chaos Soliton. Fract.*, **170** (2023), 113342. https://doi.org/10.1016/j.chaos.2023.113342
5. Z. Ye, H. Ji, H. Zhang, Passivity analysis of Markovian switching complex dynamic networks with multiple time-varying delays and stochastic perturbations, *Chaos Soliton. Fract.*, **83** (2016), 147–157. https://doi.org/10.1016/j.chaos.2015.11.027
6. F. Baldovin, D. Bovina, F. Camana, A. L. Stella, Modeling the non-Markovian, non-stationary scaling dynamics of financial markets, In: *Econophysics of order-driven markets*, Milano: Springer, 2011, 239–252. https://doi.org/10.1007/978-88-470-1766-5_16
7. L. Lalor, A. Swishchuk, Deep reinforcement learning in non-Markov market-making, *Risks*, **13** (2025), 40. https://doi.org/10.3390/risks13030040
8. J. Wang, Y. Chen, X. Ji, Z. Dong, M. Gao, C. S. Lai, Metaverse meets intelligent transportation system: an efficient and instructional visual perception framework, *IEEE Trans. Intell. Transp.*, **25** (2024), 14986–15001. https://doi.org/10.1109/TITS.2024.3398586
9. A. Mushtaq, I. U. Haq, M. A. Sarwar, A. Khan, W. Khalil, M. A. Mughal, Multi-agent reinforcement learning for traffic flow management of autonomous vehicles, *Sensors*, **23** (2023), 2373. https://doi.org/10.3390/s23052373
10. A. Ali, Y. Zhu, M. Zakarya, Exploiting dynamic spatio-temporal graph convolutional neural networks for citywide traffic flows prediction, *Neural Networks*, **145** (2022), 233–247. https://doi.org/10.1016/j.neunet.2021.10.021
11. A. Ali, H. Y. Naeem, A. Sharafian, L. Qiu, Z. Wu, X. Bai, Dynamic multi-graph spatio-temporal learning for citywide traffic flow prediction in transportation systems, *Chaos Soliton. Fract.*, **199** (2025), 116898. https://doi.org/10.1016/j.chaos.2025.116898
12. A. Ali, A. Sharafian, H. Y. Naeem, M. Zakarya, Z. Wu, X. Bai, Advanced computational models for urban traffic flow prediction: a comprehensive review and future directions, *Comput. Sci. Rev.*, **60** (2026), 100886. https://doi.org/10.1016/j.cosrev.2025.100886
13. A. Ali, R. Ali, M. Asad, L. Yang, T. Alsarhan, X. Bai, Exploiting attention-driven weather-aware multimodal spatio-temporal fusion for urban traffic flow prediction, *Future Gener. Comput. Syst.*, **183** (2026), 108559. https://doi.org/10.1016/j.future.2026.108559
14. X. Yang, J. Cao, J. Lu, Synchronization of randomly coupled neural networks with Markovian jumping and time-delay, *IEEE Trans. Circuits I*, **60** (2013), 363–376. https://doi.org/10.1109/TCSI.2012.2215804

15. J. Tao, Z. Wu, Z. Xiao, H. Rao, Y. Xu, P. Shi, Synchronization of Markov jump neural networks with communication constraints via asynchronous output feedback control, *IEEE Trans. Neur. Net. Lear.*, **35** (2024), 15724–15734. https://doi.org/10.1109/TNNLS.2023.3289297

16. Z.-G. Wu, P. Shi, H. Su, J. Chu, Stochastic synchronization of Markovian jump neural networks with time-varying delay using sampled data, *IEEE Trans. Cybernetics*, **43** (2013), 1796–1806. https://doi.org/10.1109/TSMCB.2012.2230441

17. J. Wang, Z. Wang, X. Chen, J. Qiu, Synchronization criteria of delayed inertial neural networks with generally Markovian jumping, *Neural Networks*, **139** (2021), 64–76. https://doi.org/10.1016/j.neunet.2021.02.004

18. H. Shen, S. Jiao, J. Cao, T. Huang, An improved result on sampled-data synchronization of Markov jump delayed neural networks, *IEEE Trans. Syst. Man Cyber. A*, **51** (2021), 3608–3616. https://doi.org/10.1109/TSMC.2019.2931533

19. X. Li, X. Yang, S. Song, Lyapunov conditions for finite-time stability of time-varying time-delay systems, *Automatica*, **103** (2019), 135–140. https://doi.org/10.1016/j.automatica.2019.01.031

20. H. Liu, J.-A. Lu, J. Lü, D. J. Hill, Structure identification of uncertain general complex dynamical networks with time delay, *Automatica*, **45** (2009), 1799–1807. https://doi.org/10.1016/j.automatica.2009.03.022

21. Y. Sun, J. Cao, Stabilization of stochastic delayed neural networks with Markovian switching, *Asian J. Control*, **10** (2008), 327–340. https://doi.org/10.1002/asjc.26

22. G. Li, J. Wang, K. Shi, Y. Tang, Some novel results for DNNs via relaxed Lyapunov functionals, *Math. Model. Control*, **4** (2024), 110–118. https://doi.org/10.3934/mmc.2024010

23. C.-K. Zhang, Y. He, M. Wu, Exponential synchronization of neural networks with time-varying mixed delays and sampled-data, *Neurocomputing*, **74** (2010), 265–273. https://doi.org/10.1016/j.neucom.2010.03.020

24. A. J. Abougarair, M. K. Aburakhis, M. M. Edardar, Adaptive neural networks based robust output feedback controllers for nonlinear systems, *International Journal of Robotics and Control Systems*, **2** (2022), 37–56. https://doi.org/10.31763/ijrcs.v2i1.523

25. F. Liu, Y. Yang, F. Wang, L. Zhang, Synchronization of fractional-order reaction–diffusion neural networks with Markov parameter jumping: asynchronous boundary quantization control, *Chaos Soliton. Fract.*, **173** (2023), 113622. https://doi.org/10.1016/j.chaos.2023.113622

26. X. Wu, Z. Wang, W. Lu, On time-varying delayed stochastic differential systems with non-Markovian switching parameters, *IEEE Trans. Automat. Contr.*, **69** (2024), 8908–8915. https://doi.org/10.1109/TAC.2024.3420549

27. K. Tiwari, D. Senapati, Stochastic FitzHugh–Nagumo neuron model with Gamma distributed delay kernel, *Chaos Soliton. Fract.*, **196** (2025), 116378. https://doi.org/10.1016/j.chaos.2025.116378

28. Z.-X. Ma, J. Valero, J.-C. Zhao, Multi-valued perturbations on stochastic evolution equations driven by fractional brownian motions, *Nonlinearity*, **36** (2023), 6152–6176. https://doi.org/10.1088/1361-6544/ad00f8

29. P.-T. Nguyen, B. Q. Tang, Well-posedness for fractional reaction-diffusion systems with mass dissipation in $\mathbb{R}^N$, *Nonlinearity*, **38** (2025), 115014. https://doi.org/10.1088/1361-6544/ae1d07

30. S. Guedim, A. Benkerrouche, M. S. Souid, A. Amara, J. Rashid, I. Ahmad, Initial value problem for fractional differential equations of variable order, *Math. Model. Control*, **5** (2025), 379–389. https://doi.org/10.3934/mmc.2025026

31. I. Stamova, C. Spirova, G. Stamov, Lipschitz stability analysis of fractional-order gene regulatory networks with impulsive perturbations and distributed delays, *Math. Model. Control*, **5** (2025), 421–431. https://doi.org/10.3934/mmc.2025030

32. M. I. Liaqat, A. Akgul, J. A. Conejero, Analysis of fractional stochastic systems driven by fractional Brownian motion with general memory kernel, *AIMS Math.*, **11** (2026), 1354–1381. https://doi.org/10.3934/math.2026058

33. X. Tan, W. He, J. Cao, T. Huang, Stabilization and synchronization of neural networks via impulsive adaptive control, *IEEE Trans. Neur. Net. Lear.*, **35** (2024), 15517–15527. https://doi.org/10.1109/TNNLS.2023.3287997

34. C. Li, W. Wang, Optimal impulse control and impulse game for continuous-time deterministic aystems: a review, *Artificial Intelligence Science and Engineering*, **1** (2025), 208–219. https://doi.org/10.23919/AISE.2025.000014

35. Y. Wang, J. Zhao, Neural-network-based event-triggered sliding mode control for networked switched linear systems with the unknown nonlinear disturbance, *IEEE Trans. Neur. Net. Lear.*, **34** (2023), 3885–3896. https://doi.org/10.1109/TNNLS.2021.3119665

36. H. Zhang, Y. Huang, N. Zhao, P. Shi, Improved event-triggered adaptive neural network control for multi-agent systems under denial-of-service attacks, *Artificial Intelligence Science and Engineering*, **1** (2025), 122–133. https://doi.org/10.23919/AISE.2025.000009

37. L. Zhou, J. Hu, B. Li, Partial-nodes-based state estimation for complex networks under hybrid attacks: a dynamic event-triggered approach, *Math. Model. Control*, **5** (2025), 202–215. https://doi.org/10.3934/mmc.2025015

38. S. Shanmugam, R. Vadivel, S. Sabarathinam, P. Hammachukiattikul, N. Gunasekaran, Enhancing synchronization criteria for fractional-order chaotic neural networks via intermittent control: an extended dissipativity approach, *Math. Model. Control*, **5** (2025), 31–47. https://doi.org/10.3934/mmc.2025003

39. X. Zhou, J. Cao, Z.-H. Guan, X. Wang, F. Kong, Fast synchronization control and application for encryption-decryption of coupled neural networks with intermittent random disturbance, *Neural Networks*, **176** (2024), 106404. https://doi.org/10.1016/j.neunet.2024.106404

40. Z. Cao, Y. An, Y. Wang, Y. Bai, T. Zhao, C. Zhai, Energy consumption of intermittent ventilation strategies of different air distribution modes for indoor pollutant removal, *J. Build. Eng.*, **69** (2023), 106242. https://doi.org/10.1016/j.jobe.2023.106242

41. C. Li, G. Feng, X. Liao, Stabilization of nonlinear systems via periodically intermittent control, *IEEE Trans. Circuits II*, **54** (2007), 1019–1023. https://doi.org/10.1109/TCSII.2007.903205

42. S. A. Samy, P. Durairaj, A. Ali, Z. Wu, J. Li, X. Bai, Secure fuzzy-based $H_\infty$ consensus control for nonlinear multi-agent systems under quantized sampled-data mechanism and its applications, *Eng. Appl. Artif. Intel.*, **162** (2025), 112715. https://doi.org/10.1016/j.engappai.2025.112715

43. H. Chen, P. Shi, C.-C. Lim, Exponential synchronization for Markovian stochastic coupled neural networks of neutral-type via adaptive feedback control, *IEEE Trans. Neur. Net. Lear.*, **28** (2017), 1618–1632. https://doi.org/10.1109/TNNLS.2016.2546962

44. W. Zhou, Q. Zhu, P. Shi, H. Su, J. Fang, L. Zhou, Adaptive synchronization for neutral-type neural networks with stochastic perturbation and Markovian switching parameters, *IEEE Trans. Cybernetics*, **44** (2014), 2848–2860. https://doi.org/10.1109/TCYB.2014.2317236

45. F. Dufour, R. J. Elliott, Adaptive control of linear systems with Markov perturbations, *IEEE Trans. Automat. Contr.*, **43** (1998), 351–372. https://doi.org/10.1109/9.661591

46. S. Zhao, L. Zhao, S. Wen, L. Cheng, Secure synchronization control of Markovian jump neural networks under DoS attacks with memory-based adaptive event-triggered mechanism, *Artificial Intelligence Science and Engineering*, **1** (2025), 64–78. https://doi.org/10.23919/AISE.2025.000006

47. W. Zhou, X. Zhou, J. Yang, Y. Liu, X. Zhang, X. Ding, Exponential synchronization for stochastic neural networks driven by fractional Brownian motion, *J. Franklin I.*, **353** (2016), 1689–1712. https://doi.org/10.1016/j.jfranklin.2016.02.019

48. L. Decreusefond, A. S. Üstünel, Stochastic analysis of the fractional Brownian motion, *Potential Anal.*, **10** (1999), 177–214. https://doi.org/10.1023/A:1008634027843

49. M. Parvizian, K. Khandani, Mean square exponential stabilization of uncertain time-delay stochastic systems with fractional brownian motion, *Int. J. Robust Nonlin.*, **31** (2021), 9253–9266. https://doi.org/10.1002/rnc.5764

50. H. Pan, X. Nian, W. Gui, Synchronization in dynamic networks with time-varying delay coupling based on linear feedback controllers, *Acta Automatica Sinica*, **36** (2010), 1766–1772. https://doi.org/10.1016/S1874-1029(09)60070-7

51. Y. Li, X. Zhang, J. Zhang, J. Er, J. Cao, H. Liu, Passivity and synchronization of fractional-order coupled neural networks with multiple weights: a PD approach, *Neural Networks*, **201** (2026), 108861. https://doi.org/10.1016/j.neunet.2026.108861

52. H. Gu, P. Liu, J. Lü, Z. Lin, PID control for synchronization of complex dynamical networks with directed topologies, *IEEE Trans. Cybernetics*, **51** (2021), 1334–1346. https://doi.org/10.1109/TCYB.2019.2902810

53. J. Xiao, K. Shi, Y. Teng, J. Qi, H. Fan, Relaxed research on synchronization problem of fractional-order fuzzy octonion-valued BAM neural networks by the non-decomposition method on the high-dimension oblique field, *Fractal Fract.*, **10** (2026), 414. https://doi.org/10.3390/fractalfract10060414

54. J. Xiao, B. Huang, S. Wen, The new quadratic inequality and particle swarm optimization method for the relaxed synchronization criteria of fractional-order lower-dimension-valued bilayer neural networks, *Nonlinear Dyn.*, **114** (2026), 708. https://doi.org/10.1007/s11071-026-12599-1


AIMS Press